CIRP Annals - Manufacturing Technology 00 (2025) 1–5

Contents lists available at ScienceDirect

CIRP Annals - Manufacturing Technology

journal homepage: https://www.editorialmanager.com/CIRP/default.aspx

Multiscale optical surface integrating multifocal imaging and wavelength filtering for compact snapshot spectral imaging

Xinquan Zhang (2)[a,#], Yaoke Wang[b,#], Hao Wu[a], Limin Zhu[a], Ping Guo (2)[b,*]

[a] School of Mechanical Engineering, Shanghai Jiao Tong University, Shanghai, 200240, China
[b] Department of Mechanical Engineering, Northwestern University, Evanston, IL 60208, USA

ARTICLE INFO

Article history:
Available online xxx

Keywords:
Optical
Ultra-precision
Spectral imaging

ABSTRACT

Snapshot spectral imaging enables single-exposure acquisition of spectral images but is constrained by bulky designs and compromised spatial resolutions. This study presents a multiscale optical surface that integrates macro-scale structures for multifocal imaging and micro-scale staircases for wavelength filtering into a unified ultra-compact form. The design employs a multiscale framework grounded in Fourier optics and is fabricated using ultra-precision diamond turning. Validation experiments demonstrate the system's ability to capture discrete spectral images using only a single optical component, with measured spectral characteristics closely matching theoretical predictions. This new design provides a compact and cost-effective solution for diverse spectral imaging applications.

1. Introduction

Spectral imaging systems produce images containing precise spectral information, surpassing the capabilities of conventional cameras that are limited to RGB outputs. These systems find extensive applications across various fields, such as remote sensing, astronomy, and biomedical engineering [1].

Spectral imaging systems are generally categorized into two types: scanning-based and snapshot-based systems [1]. Snapshot spectral imaging systems capture multiple-channel spectral images in a single exposure without requiring scanning. While these systems are ideal for high-speed and real-time applications, they present significant challenges in optical design. Among the popular snapshot imaging techniques [2], both coded aperture methods [3,4] and lenslet arrays [5] can achieve hyperspectral-level bandwidth but often require post-processing or compromise spatial resolution. In contrast, the spectral sampling method, such as prism-based [6] or filter-array-based [7] approaches, generates complete images at specific wavelengths without reducing spatial resolution. Nevertheless, this approach typically requires multiple optical components with diverse functions to perform wavelength filtering and image focusing, which often results in bulky systems and limits their suitability for portable applications. The "Mosaic-array" imaging sensor [8] or integrated filter array [9] offers a compact alternative but remains expensive and lacks compatibility with standard CCD/CMOS sensors or direct human-eye observation. The meta-lens-based design [10] offers extreme compactness but is limited to clean room production and is challenging to replicate due to its multi-layer structure. Ultimately, existing snapshot spectral imaging solutions face a persistent trade-off between system complexity, cost, and the need for multi-step post-processing.

In this study, we propose an ultra-compact multiscale optical surface that simultaneously achieves wavelength filtering and discretized imaging in a single optical component, eliminating the need for post-processing. Specifically, our design integrates wavelength filtering and discretized imaging into a surficial structure with an extremely thin profile ($<30\ \mu$m),making it as portable as a coin and requiring no additional optical devices. The optical surface integrates macro-scale structures, which enable multifocal imaging similar to a specular freeform mirror, with micro-scale staircase structures that filter wavelengths into distinct band-pass ranges. Notably, the staircase design of the micro-scale structures realizes the wavelength filtering using zero-order diffraction exclusively at the specular angle. Our design is the first attempt at using diffractive optics for one-step multispectral imaging, with a single-layer surficial structure that enables easy replication when served as an optical mold. A cross-scale optical design method is introduced, where macro- and micro-scale structures are designed separately based on Fresnel diffraction in Fourier optics [11] and then integrated into a single optical component. More importantly, this design represents the first all-in-one snapshot spectral imaging solution in an ultra-compact surficial format.

To fabricate the proposed multiscale optical surface, ultra-precision diamond turning is employed as the preferred method for mass production due to its ability to provide deterministic material removal across different scales [12]. It has also demonstrated feasibility in machining microstructures [13], freeform surfaces [14], and high-aspect-ratio structures [15]. In this study, a spiral tool path is generated through synchronized servo axis motions, guiding the diamond tool to create the multiscale optical structure with high precision. The resultant machined surface is consistent with the multiscale design in both macro- and micro-scales. An optical setup is constructed to validate the surface's optical performance. Using a standard imaging sensor, four discrete images are successfully captured, and the spectral characteristics of each image align with theoretical predictions when measured by a

* Corresponding author.
E-mail address: ping.guo@northwestern.edu (P. Guo).
# These authors have equal contribution to this work.

https://doi.org/10.1016/j.cirp.2025.03.025

Please cite this article as: X. Zhang et al., Multiscale optical surface integrating multifocal imaging and wavelength filtering for compact snapshot spectral imaging, CIRP Annals - Manufacturing Technology (2025), https://doi.org/10.1016/j.cirp.2025.03.025

spectrometer. Due to the surficial design, the introduced multiscale optical surface offers a compact, cost-effective, and scalable solution for future spectral imaging applications.

2. Design of the multiscale optical surface

The multispectral imaging device is designed to perform two essential functions: first, achieving wavelength selectivity by splitting light into different bandwidths; and second, focusing light beams for individual imaging for each bandwidth. To enable an ultra-compact and scalable design, we propose integrating these two optical functions into a single multiscale optical surface. In this design, the macro-scale structures, which are significantly larger than the wavelength of visible light, focus light beams onto sub-images at different focal points. Simultaneously, diffractive micro-scale structures embedded on the macro-scale surfaces filter each sub-image to isolate specific bandwidths. This new approach enables the display of multiple sub-images, each corresponding to a distinct target bandwidth, using a single optical device, as illustrated in Fig. 1.

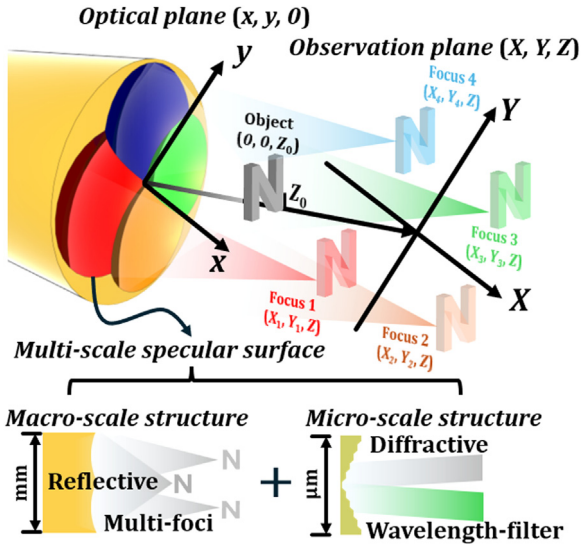

Fig. 1. Multi-spectral imaging by multiscale optical structures.

As illustrated in Fig. 1, we analyze the light beam originating from the object (represented by the gray "N" for Northwestern) positioned at (*0, 0, Z_0*), with a wavefront distribution $U_0(x, y)$ incident on the optical plane. The resulting intensity distribution on the observation plane, located at a distance Z is $I(X, Y)$. The propagation of light can be uniformly described using Fresnel diffraction [11] under paraxial conditions:

$$I(X,Y) = I_0 e^{j\frac{\pi}{Z\lambda}(X^2+Y^2)} \left\| \mathscr{F}\left\{ U_0(x,\ y) e^{-j\frac{4\pi h(x,y)}{\lambda}} e^{j\frac{\pi}{Z\lambda}(x^2+y^2)} \right\} \right\|, \tag{1}$$

where λ is the wavelength; $h(x, y)$ represents the surface profile; I_0 is a constant for given λ and Z, and $\mathscr{F}$ denotes the Fourier transform. Assuming that the surface profile $h(x, y)$ is composed of the macro-scale structure $h_a(x, y)$ and micro-scale structure $h_b(x, y)$, then the convolution theorem can be applied to decouple their contributions in the intensity equation as:

$$I(X,Y) = I_0 e^{j\frac{\pi}{Z\lambda}(X^2+Y^2)} \left\| \mathscr{F}\left\{ U_0(x,\ y) e^{-j\frac{4\pi h_a(x,y)}{\lambda}} e^{j\frac{\pi}{Z\lambda}(x^2+y^2)} \right\} * \mathscr{F}\left\{ e^{-j\frac{4\pi h_b(x,y)}{\lambda}} \right\} \right\| \tag{2}$$

In Eq. (2), the intensity distribution induced by the hierarchical optical structures is separated into the convolution of Fourier transforms related to the macro-scale and micro-scale structure, respectively. This decoupling allows the independent design of optical structures at each scale.

2.1. Design of the micro-scale structure for wavelength filtering

The wavelength selectivity effect requires precise manipulation of light at the wavelength level, which is achieved through micro-scale structures. Here, we propose a staircase ring structure, as illustrated in Fig. 2a to achieve zero-order diffraction for wavelength filtering. This structure consists of concentric stairs with periodic profiles along the radial direction. Each step is designed with a width of 3 μm to ensure machinability, while the height of each step is set to half the target wavelength λ_0. This design selectively retains light with a wavelength approximately twice the step height, effectively filtering out light of other wavelengths. For instance, if the target wavelength is 560 nm (green light), the step height would be 280 nm.

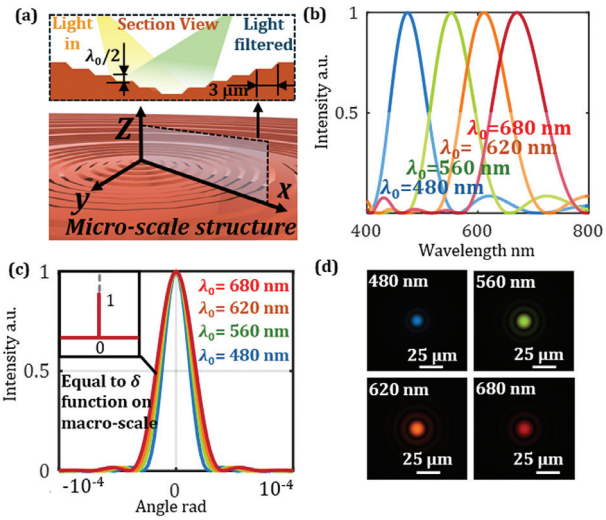

Fig. 2. (a) Staircase ring structure design of the micro-scale structure; (b) simulated spectrum induced by the structures of different λ_0 and (c) corresponding angular distribution; (d) simulated images of a point light source focused at Z = 800 mm.

Under the concentric (axial-symmetric) assumption, the intensity distribution purely induced by the micro-scale structure I_b can be written by:

$$I_b(X,\ Y) = \left\| \mathscr{F}\left\{ e^{-j\frac{4\pi h_b(r)}{\lambda}} \right\} \right\| = \left\| 2\pi \int_0^R e^{-j\frac{4\pi h_b(r)}{\lambda}} J_0\left(2\pi \frac{\sqrt{X^2+Y^2}}{\lambda Z} r \right) r\, dr \right\|. \tag{3}$$

Here, $r = \sqrt{x^2+y^2}$. J_0 represents the first-kind Bessel function, and R denotes the radius of the outer ring in the concentric structure. A MATLAB program was developed to simulate the optical performance of the micro-scale structures, with the simulation parameters listed in Table 1.

Table 1
Simulation parameters for micro-scale structures.

Number of steps		Step width
5		3 μm
Wavelength λ	Objective distance Z_0	Image distance Z
400 to 700 nm	200 mm	800 mm

Simulation results presented in Fig. 2b demonstrate that the micro-scale structure functions as an effective wavelength-selective filter. As depicted in Fig. 2c, the intensity distribution, where the angle is denoted by r/Z, shows a significant value only near the zero point. This structure does not alter the orientation of the light beam but instead filters the optical spectrum. Then, assume that the micro-scale structure is illuminated by a point light source and the light is focused at Z = 800 mm, a set of dots corresponding to different wavelengths is observed, as shown in Fig. 2d. This behavior indicates that the micro-scale structure functions as a wavelength-filtering specular reflector, eliminating high-order diffraction. Therefore, for practical applications, the optical behavior of the micron-scale structure can be approximated as a delta function, where light intensity depends solely on the wavelength.

Because the convolution of any function with a delta function yields the function itself, the optical performance of the macro-scale structure then can be designed independently of the micro-scale structure.

Please cite this article as: X. Zhang et al., Multiscale optical surface integrating multifocal imaging and wavelength filtering for compact snapshot spectral imaging, CIRP Annals - Manufacturing Technology (2025), https://doi.org/10.1016/j.cirp.2025.03.025

2.2. Design of the macro-scale structure for multifocal imaging

The optical function of the macro-scale structure is to focus the image onto multiple points. To achieve this, the macro-scale structure is divided into four quadrants, as illustrated in Fig. 3. The radius R of each quadrant is 5 mm. Given the object point $(0, 0, Z_0)$, each quadrant is assigned an individual focus point (X_i, Y_i, Z), where i ranges from 1 to 4. Furthermore, by rewriting the macro-scale component of Eq. (2), the intensity distribution induced by the macro-structure can be represented by:

$$I_a(X,Y) = I_0 \left\| \iint_{\Omega} e^{j\frac{4\pi}{\lambda}\left(-h(x,y)+\frac{(x-X)^2+(y-Y)^2}{4Z}+\frac{x^2+y^2}{4Z_0}\right)} dxdy \right\|, \quad (4)$$

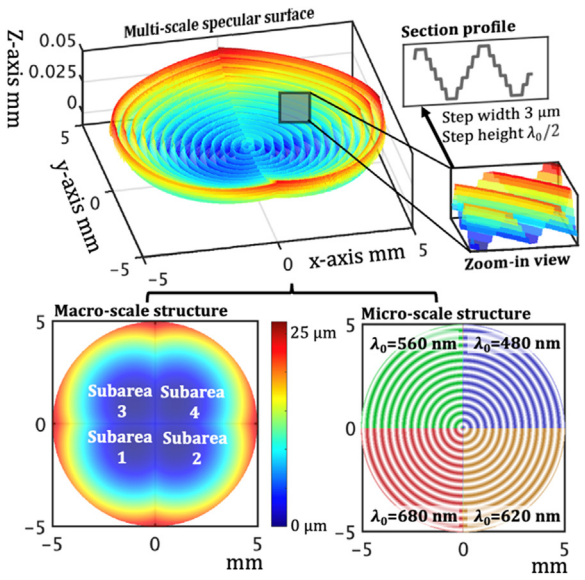

Fig. 3. Integration of macro- and micro-scale structures of four quadrants into the multiscale optical surface.

where Ω represents the area of interest. To focus the light beam onto the focus point (X_i, Y_i, Z), the surface profile $h_a(x, y)$ is determined by the following solution:

$$h_a(x,y) = \frac{(x-X_i)^2+(y-Y_i)^2}{4Z} + \frac{x^2+y^2}{4Z_0}. \quad (5)$$

The macro-scale surface profile is calculated using the parameters listed in Table 2 and consists of four quadrants. Each quadrant is assigned a specific target wavelength, corresponding to different micro-scale structures. The designed multiscale optical surface, integrating both the macro-scale and micro-scale structures, is illustrated in Fig. 3.

Table 2
Parameters of four quadrants of different target wavelengths.

Quadrant 1	Quadrant 2	Quadrant 3	Quadrant 4
Focus (X_1, Y_1) $(5, 5)$ mm	Focus (X_2, Y_2) $(-5, 5)$ mm	Focus (X_3, Y_3) $(5, -5)$ mm	Focus (X_4, Y_4) $(-5, -5)$ mm
Target wavelength λ_0 480 nm	Target wavelength λ_0 560 nm	Target wavelength λ_0 620 nm	Target wavelength λ_0 680 nm

3. Fabrication of hierarchical optical structures

We employ a three-axis tool path generation algorithm (C, X, Z), incorporating constant angle discretization and Steady X tool radius compensation. The coordinate configuration is shown in Fig. 4a. In contrast to traditional planning, our tool servo turning defines the path control points for the servo axes in a spiral pattern, as illustrated in Fig. 4b. This spiral path is created by combining the radial feed motion of the X-axis with the tangential feed motion of the C-axis. The cutting depth of the diamond tool along this path is adjusted by the reciprocating motion of the Z-axis. Therefore, the tool trajectory

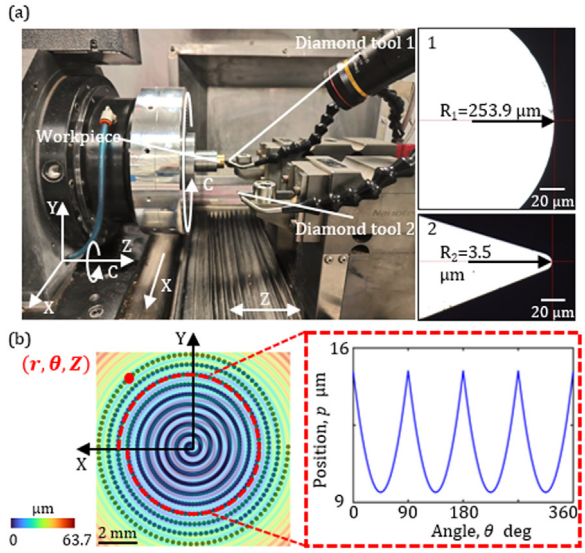

Fig. 4. (a) Experimental setup and (b) tool path generation method for turning of the multiscale optical surface.

points in polar coordinates (r, θ, z) can be described as follows:

$$\begin{cases} r(n) = R - f_s n \Delta t \\ \theta(n) = 2\pi w_C n \Delta t \\ z(n) = \hbar(r(n), \theta(n)) \end{cases}, \quad (6)$$

where n is the path index number; R represents the radius of the fabricated surface; f_s is the feed rate of the spiral path; Δt denotes the time interval; w_C is the rotary speed of the C-axis; $\hbar$ is a function of the Steady X compensation [16] dependent on the diamond tool radius and the target surface.

Diamond turning experiments were conducted on a commercial tri-axis ultra-precision machine tool (250UPL, *Nanotech*, USA), as shown in Fig. 4a. A brass workpiece was mounted on the C-axis, while two diamond turning tools were attached to the Z-axis. The macro-scale structure of the substrate surface was machined using a round tool with a 254 μm radius, whereas the micro-scale structure was created using a round tool with a 3.5 μm radius. For the finishing cut of the micro-scale structure, a spiral tool path was commanded with a rotary speed of 83 RPM, a feed rate of 0.5 μm/r, and an angular interval of 0.5°

4. Experimental result

The exemplary multiscale optical surface was fabricated using the parameters outlined in Tables 1 and 2, and the resulting workpiece was examined under a digital microscope (VHX-X1, *Keyence*, Japan). At 20 × magnification, the entire machined area is displayed, as shown in Fig. 5a. The moiré pattern observed at the transition zones between different micro-scale structures highlights the boundaries of different quadrants. At 1000 × magnification, the microscopic image reveals the central portion of the fabricated micro-scale structures, displaying a concentric, periodic staircase pattern with a clean surface finish, as intended.

To evaluate the accuracy of the macro-scale structure, a white-light profilometer (NewView 7300, *Zygo*, USA) was used to measure the workpiece. The measured surface profile, shown in Fig. 5b, closely aligns with the desired morphology depicted in Fig. 3. At higher magnifications, aliased micro-scale structures become visible as their dimensions approach the diffraction limit of the microscope. The global forming error, derived by comparing the measured profile with the theoretical profile represented by Eq. (5), is illustrated in Fig. 5c. The error remains within 2 μm and is likely caused by aliased micro-scale structures, measurement stitching errors, and errors in the turning process.

To validate the formation of the micro-scale structures, atomic force microscopy (AFM) tests were performed on randomly selected areas within each subarea, with the results shown in Fig. 5d. The AFM image presents an exemplary depth map for a structure where λ_0 is 620 nm and the measured profiles reveal a staircase pattern with a

Please cite this article as: X. Zhang et al., Multiscale optical surface integrating multifocal imaging and wavelength filtering for compact snapshot spectral imaging, CIRP Annals - Manufacturing Technology (2025), https://doi.org/10.1016/j.cirp.2025.03.025

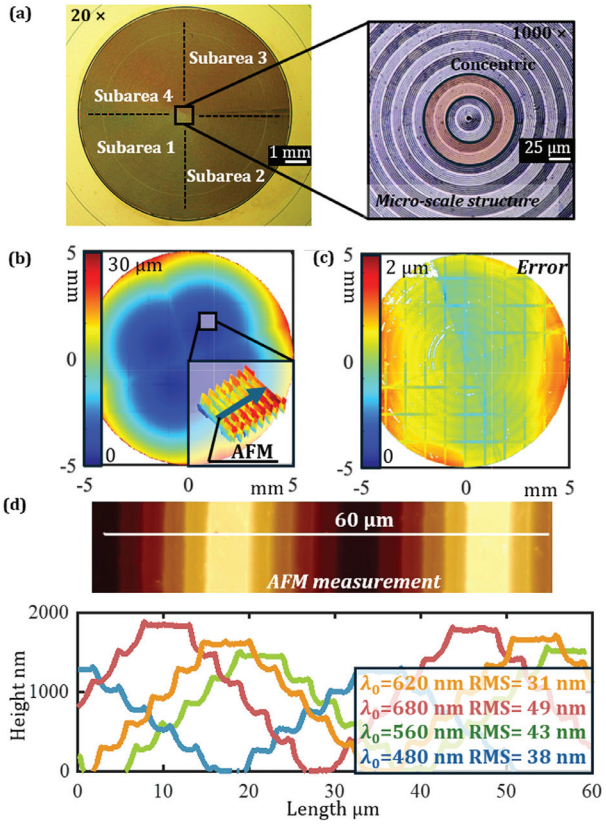

Fig. 5. (a) Microscopic images of the multiscale optical structure; (b) surface profile and (c) forming error of the machined surface; and (d) results of the AFM measurement.

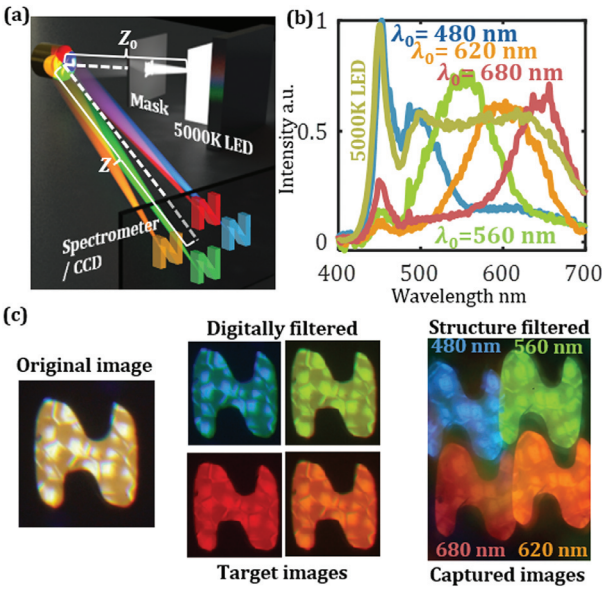

Fig. 6. (a) Setup for measurement of optical performance; (b) measured spectrum of images of different λ_0; (c) the original image, digitally filtered images, and captured spectral images using a bare digital camera without any lenses.

36-micron period and step heights incrementally increasing with λ_0 while the machined error (RMS) ranges from 31 to 49 nm.

Functional tests were performed to evaluate the optical performance of the fabricated hierarchical optical structure. The optical setup diagram is shown in Fig. 6a. A mask featuring the "N" pattern (representing Northwestern) was illuminated using a 5000 K LED light source, with the reference spectrum displayed on the right side of the figure. The original image was captured using a standard mirror without wavelength-selective properties, serving as a baseline case. The illuminated mask acted as the object, while the machined optical surface focused and filtered the light from the object, projecting four focused images, each corresponding to a specific wavelength range, onto the spectrometer or the imaging sensor plane.

When measured using a spectrometer (CCS200, *Thorlabs*, USA), the spectra of the four focused images are presented in Fig. 6b. Compared to the reference spectrum of the light source, the original spectrum is successfully split into four distinct portions with the central wavelengths designed at 480, 560, 620, and 680 nm, respectively. The bandwidths (−3 dB threshold) are measured to be 42 nm, 64 nm, 77 nm, and 52 nm, while the RMS similarity to the simulated spectrums (source spectrum considered) is 89.6%, 90.3%, 86.0%, and 84.1%, respectively. Additionally, the spectral images are directly projected to the CMOS sensor of a digital camera (α7, *Sony*, Japan) without using any additional lenses from the camera. The spatial resolution of the spectral imaging system, measured using the camera, is 4.8 μm/pixel after magnification by the surface. The results validate that the "N" pattern is individually focused onto four distinct locations, selectively displaying the target wavelength information as spectral images. Fig. 6c presents a direct comparison of original images and digitally filtered (spectrum in Fig. 2b applied) results with the captured spectral images. The captured images show consistent color tones and outlines with the original images.

The object size is currently restricted to 2.5 mm to prevent undesired oversampling in the demonstrated design. However, it can be adjusted by modifying the focus points. Ghosting in the image arises from machining errors in micro-scale structures, leading to light energy diffusion, while macro-scale errors cause imperfect focusing. The current design includes four channels, with the flexibility to expand by incorporating additional subareas. The bandwidth, presently limited to approximately 50 nm, can be further narrowed by increasing the steps in micro-scale structures.

5. Conclusion

We propose a multiscale optical surface that offers a compact and cost-effective solution for snapshot spectral imaging by integrating macro-scale structures for multifocal imaging and micro-scale structures for wavelength filtering. These micro- and macro-scale features are seamlessly combined into a single surficial optical surface, with an optical structure height of less than 30μm. Fabricated using ultra-precision diamond turning, the multiscale optical surface demonstrated high forming accuracy and clean finishes at both scales. Validation experiments confirm its ability to split the reference spectrum into four distinct bands and project focused spectral images onto an imaging sensor without requiring additional optical components. The design presented in this study demonstrates the generation of four distinct spectral images. The number of spectral bands can be further extended by applying the same design concept, dividing additional subareas with different target wavelengths, and compensating for the light intensity loss by enlarging the optical radius. In conclusion, our design represents the first all-in-one snapshot spectral imaging solution in an ultra-compact surficial format, paving the way for future solutions in diverse spectral imaging applications.

Declaration of competing interest

The authors declare that they have no known competing financial interests or personal relationships that could have appeared to influence the work reported in this paper.

CRediT authorship contribution statement

Xinquan Zhang: Writing – original draft, Methodology, Investigation, Funding acquisition. **Yaoke Wang:** Writing – original draft, Validation, Methodology, Investigation, Formal analysis, Conceptualization. **Hao Wu:** Writing – review & editing, Methodology, Investigation. **Limin Zhu:** Writing – review & editing, Supervision, Resources, Funding acquisition. **Ping Guo:** Writing – review & editing, Supervision, Resources, Funding acquisition, Conceptualization.

Please cite this article as: X. Zhang et al., Multiscale optical surface integrating multifocal imaging and wavelength filtering for compact snapshot spectral imaging, CIRP Annals - Manufacturing Technology (2025), https://doi.org/10.1016/j.cirp.2025.03.025

References

[1] Hagen N, Kudenov MW (2013) Review of snapshot spectral imaging technologies. *Optical Engineering* 52/9:090901.
[2] Ding K, Wang M, Chen M, Wang X, Ni K, Zhou Q, Bai B (2024) Snapshot Spectral imaging: from spatial-spectral mapping to metasurface-based imaging. *Nanophotonics* 13/8:1303–1330.
[3] Arguello H, Pinilla S, Peng Y, Ikoma H, Bacca J, Wetzstein G (2021) Shift-variant color-coded diffractive spectral imaging system. *Optica* 8/11:1424–1434.
[4] Song L, Wang L, Kim MH, Huang H (2022) High-accuracy image formation model for coded aperture snapshot spectral imaging. *IEEE Transactions on Computational Imaging* 8/:188–200.
[5] Dwight JG, Tkaczyk TS (2017) Lenslet array tunable snapshot imaging spectrometer (Latis) for hyperspectral fluorescence microscopy. *Biomedical Optics Express* 8/3:1950–1964.
[6] Greiner J, Laux U (2022) A novel compact 4-channel beam splitter based on a Kösters-Type prism. *CEAS Space Journal* 14/2:253–260.
[7] Murakami Y, Yamaguchi M, Ohyama N (2012) Hybrid-resolution multispectral imaging using color filter array. *Optics Express* 20/7:7173–7183.
[8] Geelen B, Tack N, Lambrechts A (2014) *A Compact Snapshot Multispectral Imager with a Monolithically Integrated Per-Pixel Filter Mosaic. Advanced fabrication technologies for micro/nano optics and photonics VII*, SPIE, San Francisco, CA80–87.
[9] Wang S-W, Xia C, Chen X, Lu W, Li M, Wang H, Zheng W, Zhang T (2007) Concept of a high-resolution miniature spectrometer using an integrated filter array. *Optics Letters* 32/6:632–634.
[10] Hua X, Wang Y, Wang S, Zou X, Zhou Y, Li L, Yan F, Cao X, Xiao S, Tsai DP (2022) Ultra-compact snapshot spectral light-field imaging. *Nature Communications* 13/1:2732.
[11] Goodman JW (2005) *Introduction to Fourier Optics*, Roberts and Company publishers Englewood, CO.
[12] Brinksmeier E, Karpuschewski B, Yan J, Schönemann L (2020) Manufacturing of multiscale structured surfaces. *CIRP Annals* 69/2:717–739.
[13] Wu H, Zhang X, Zhu L, Ren M, Rahman M (2024) Parallel tool servo turning of microstructured surfaces. *CIRP Annals* .
[14] Fang F, Zhang X, Weckenmann A, Zhang G, Evans C (2013) Manufacturing and measurement of freeform optics. *Cirp Annals* 62/2:823–846.
[15] Zhang X, Li Z, Zhang G (2018) High performance ultra-precision turning of large-aspect-ratio rectangular freeform optics. *CIRP Annals* 67/1:543–546.
[16] You K, Yan G, Fang F, Li Z, Zhang Y (2020) Tool path generation of turning optical freeform surfaces using arbitrary rake angle tools. *Optics Express* 28/25:38252–38266.

Please cite this article as: X. Zhang et al., Multiscale optical surface integrating multifocal imaging and wavelength filtering for compact snapshot spectral imaging, CIRP Annals - Manufacturing Technology (2025), https://doi.org/10.1016/j.cirp.2025.03.025